Agricultural and Forest Meteorology 359 (2024) 110267

Contents lists available at ScienceDirect

Agricultural and Forest Meteorology

journal homepage: www.elsevier.com/locate/agrformet

LiDAR insights on stand structure and topography in mountain forest wind extreme events: The Vaia case study

Michele Torresani [a,*], Leonardo Montagnani [a], Duccio Rocchini [b,c], Vítězslav Moudrý [c], Andrea Andreoli [a], Camilla Wellstein [a,d], Kenta Koyanagi [a], Luca Da Ros [a], Giovanni Bacaro [e], Michela Perrone [c], Chiara Salvatori [a,f], Irene Menegaldo [a], Enrico Guatelli [g], Roberto Tognetti [a]

[a] *Free University of Bozen/Bolzano, Faculty of Agricultural, Environmental and Food Sciences, Piazza Universitá/Universitätsplatz 1, 39100, Bozen/Bolzano, Italy*
[b] *BIOME Lab, Department of Biological, Geological and Environmental Sciences, Alma Mater Studiorum University of Bologna, Via Irnerio 42, 40126 Bologna, Italy*
[c] *Czech University of Life Sciences Prague, Faculty of Environmental Sciences, Department of Spatial Sciences, Kamýcka 129, Praha - Suchdol, 16500, Czech Republic*
[d] *Competence Center for Economic, Ecological and Social Sustainability, Free University of Bozen-Bolzano, Piazza Universitá/Universitätsplatz 1, 39100, Bozen/Bolzano, Italy*
[e] *Department of Life Sciences, University of Trieste, Via L. Giorgieri 10, 34127 Trieste, Italy*
[f] *Department of Civil, Constructional and Environmental Engineering, University of Rome 'La Sapienza', Rome, Italy*
[g] *Visual ART FEIMC, Via Dolomiti, 39100 Bolzano-Bozen, Italy*

ARTICLE INFO

Keywords:
Climate change
Extreme events
Forest
Forest structural characteristics
Remote sensing
Windstorm

ABSTRACT

With climate change intensifying, forests globally are becoming more susceptible to extreme weather events, such as windstorms, which account for a significant share of Europe's economic losses. The Vaia windstorm of late autumn 2018, striking Italy's North-East alpine ecosystem, highlighted this vulnerability, toppling over 8.5 million cubic meters of timber and sparking debates on forest management's role in mitigating such disasters. This study aims to evaluate the impact of structural and topographical characteristics on the damage caused by Vaia, using Airborne Light Detection And Ranging (LiDAR) data collected before the storm, in four heavily affected forest areas in the Italian Alps (Carezza in the Province of Bolzano-Bozen, Predazzo, Manghen, and Primiero in the Province of Trento). We analyzed structural metrics like forest height heterogeneity (HH), forest mean height, and density, alongside topographical features such as aspect, slope, and altitude, to discern their influence on the storm's severity.

Our results revealed that the most significant difference between affected and unaffected areas is forest mean height that was found higher in areas hit by the storm. Forest density played a lesser but important role, with denser areas experiencing more severe damage, though this was only significant in certain areas. Contrary to common assumptions, our analysis revealed that forest height heterogeneity (HH) did not have a significant effect on damage levels. The findings, consistent with previous research, revealed a significant association between specific aspects, particularly the South-East orientation, which aligned with the predominant wind direction during the Vaia storm, and an increased likelihood of damage.

Both structural and topographical factors interact in complex ways to influence the outcome of such extreme events. The study emphasizes the dominant impact of the Vaia windstorm, noting that while managing forest height and density may help, the diverse topography complicates these efforts. Our study explicitly tested the effectiveness of using Airborne LiDAR data to explore forest structural and topographical factors that influenced Vaia storm damage. The achieved results demonstrate that LiDAR serves as a useful tool to field data, offering valuable insights for broader applications in this domain.

1. Introduction

As climate change continues to intensify, ecosystems globally, particularly forests, are becoming more vulnerable to a range of extreme weather events (Abram et al., 2021; Seidl et al., 2017). The increasing impact of climate change is evident in a noticeable rise in both the frequency and intensity of disturbances within forest ecosystems,

* Corresponding author.
E-mail address: michele.torresani@unibz.it (M. Torresani).

https://doi.org/10.1016/j.agrformet.2024.110267
Received 19 April 2024; Received in revised form 27 September 2024; Accepted 15 October 2024
Available online 30 October 2024

including potential factors such as windstorms, forest fires, and insect infestations (Ummenhofer and Meehl, 2017). It has been estimated that, from 1980 to 2016, climate and weather-related extreme events incurred substantial economic losses, totaling €450 billion across the 33 member countries of the European Environment Agency (EEA). Among these, windstorms emerged as a significant peril in Europe, ranking second in terms of frequency, severity, and economic impact. Windstorms accounted for a notable 25% of all economic losses attributed to climatic hazards in Europe during this period (European Environment Agency, 2017).

The ramifications of wind disturbances on forest ecosystems are profound and multifaceted. One major outcome is the substantial depletion of forested regions, whose destruction not only disrupts the current ecological equilibrium but also impacts biodiversity, influencing the plant and animal species reliant on these environments (Kamp et al., 2020). In addition to ecological effects, wind disturbances lead to a decrease in the carbon absorption capacity of forests (Pilli et al., 2021), impacting their role in regulating greenhouse gas emissions. The economic toll of wind disturbances is substantial (Udali et al., 2021), affecting both the forestry industry and communities dependent on forest resources. From a social perspective, wind disturbances alter the landscape and recreational value of affected areas, the destruction of forests diminishes the aesthetic appeal and recreational opportunities, impacting both local residents and visitors. Moreover, the disruption to ecosystem services provided by forests, such as water filtration and soil stabilization (Borrelli et al., 2017), further compromises the overall well-being of communities.

In the late autumn of 2018, the Italian landscape experienced the formidable Vaia windstorm, an atmospheric tempest of unprecedented intensity (Giannetti et al., 2019, 2021; Vaglio Laurin et al., 2021). Vaia manifested as a rapid and intense low-pressure system, generating wind speeds that surpassed the threshold of conventional meteorological expectations (Vaglio Laurin et al., 2021). Originating in the Adriatic Sea, the storm carved a path of destruction as it traversed through northeastern Italy, Austria, and Slovenia. With peak wind speeds exceeding 180 km/h (Giovannini et al., 2021), Vaia's impact was felt acutely, leading to widespread infrastructure damage and, notably, severe repercussions for forested ecosystems, destroying more than 8.5 million cubic meters of wood, largely devastating the affected mountain ecosystems (Giannetti et al., 2019).

The emergence of remote sensing technologies, encompassing optical, LiDAR, and radar sensors, coupled with advancements in diverse platforms such as airborne, satellite, and UAV, has significantly transformed our capacity to detect and extract vital information essential for ecosystem monitoring (Torresan et al., 2020; Domingo et al., 2023; Rocchini et al., 2022; McKenna et al., 2023; Moudrỳ et al., 2024) such these extreme climatic events (Kuzu et al., 2024). The efficiency of these data is highlighted by its ability to rapidly cover extensive areas, offering valuable insights that would be logistically challenging and resource-intensive to obtain solely through on-the-ground surveys (Torresani et al., 2023a; Pettorelli et al., 2018). However, it is important to acknowledge that, while remote sensing information offers expedience and cost-effectiveness, there is a potential trade-off involving a reduction in accuracy compared to meticulous field data collection methods (Rocchini et al., 2019). Nevertheless, numerous studies have demonstrated the utility of remote sensing data in monitoring various forest disturbances, including wind damages (Tomppo et al., 2021; Olmo et al., 2021), forest fires (Gamze and Çorumluoğlu, 2023) droughts (Le et al., 2023) and infestations (Marvasti-Zadeh et al., 2023), further emphasizing its significance in ecosystem management.

Light Detection And Ranging (LiDAR) data, in particular, facilitates a comprehensive understanding of forest ecosystems, encompassing not only structural attributes, biodiversity metrics, and topographical features but also offering valuable insights into forest biomass, canopy height, and vegetation density (Rahman et al., 2022; Béland and Kobayashi, 2021; Du et al., 2023). This technological advancement plays a crucial role in forest management, presenting a swift and cost-effective alternative to traditional field-based data collection methods. Furthermore, LiDAR's capacity to capture detailed three-dimensional information allows for precise quantification of forest structure at both the tree and pixel levels, and assists in monitoring changes over time (Torresani et al., 2023b).

Following the Vaia windstorm, there was a prevailing notion attributing the substantial forest loss to the perceived weakness in the forest structure, a factor that could be influenced by forest management practices. In light of this, we aim to empirically test this multifaceted perspective by evaluating, by the use of LiDAR data, various forest structural variables, including height heterogeneity (HH), forest mean height and forest density, across areas both affected and unaffected by Vaia. This analysis seeks to discern the nuanced relationship between forest structure, forest management, and vulnerability to extreme events, providing valuable insights for future forest management strategies.

The study aims to investigate the impact of the Vaia windstorm in four heavily affected forest areas in the Italian Alps (Carezza in the Province of Bolzano-Bozen, Predazzo, Manghen, and Primiero in the Province of Trento) utilizing LiDAR data to analyze structural variables such as HH, forest mean height and forest density. By comparing storm-affected areas with nearby unaffected regions, the study seeks to discern any significant differences in forest structure. Additionally, we endeavored to provide a comprehensive response to the loss of forest by employing LiDAR data to extract information on topographic information such as aspect, slope, and altitude of both the areas affected and unaffected.

2. Material and methods

2.1. Study areas

Four study areas (Table 1), each covering approximately 5500 ha, situated in Italy within the Province of Trento and Bolzano-Bozen, which were significantly impacted by the Vaia Windstorm, were chosen for this investigation (Fig. 1). The selection of these areas was based on the availability of Airborne Laser Scanning (ALS) LiDAR data.

The first study area, named "Carezza", is situated in the Province of Bolzano-Bozen, nestled at the North side of the Latemar mountain range. This mountainous terrain encompasses elevations ranging from approximately 1000 m a.s.l. to 2800 m a.s.l.. The landscape is characterized by diverse valleys, each presenting unique aspects and slopes that span from undulating to moderately steep, aligning with the slope gradient classifications of the USDA (United States Department of Agriculture). The forest area is 3400 ha of which 450 ha hit by Vaia storm.

The second study area, called "Predazzo" is located in the Province of Trento, nearby the municipality of Predazzo at the South side of the Latemar mountain range. This area is also characterized by mountainous terrain encompassing elevations ranging from approximately 980 m a.s.l. to 2400 m a.s.l.. Also this area is characterized by the presence of diverse valleys, having different aspects and slopes that, as in the Carezza area, span from undulating to moderately steep. The forest area is 3500 ha of which 900 ha hit by Vaia storm.

The third area "Manghen" is located near the Manghen pass, in the North-East part of the Trento Province, in between Fiemme valley and Valsugana. The forest area is around 5100 ha of which 730 ha hit by Vaia storm. The geographical features of this region include mountainous terrain, with elevations ranging from approximately 700 m a.s.l. to 2400 m a.s.l..

Finally the fourth area "Primiero", is located within the Primiero valley, at the West side of the Trento Province at the foothill of the "Pale di San Martino" dolomites ridge. The forested area is almost 4000 ha of which 660 ha hit by the Vaia storm. Also this area is characterized

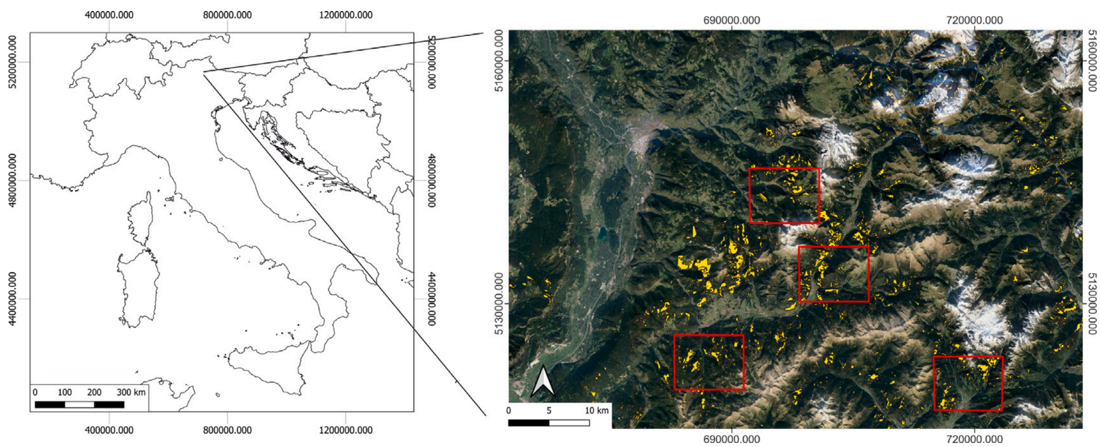

Fig. 1. In red, the border of the four study areas situated in the Italian Alps within the Province of Trento and Bolzano-Bozen. In yellow the FORWIND dataset indicating the forested areas hit by the Vaia storm. Background image used: Google Image at February 20th 2024. Coordinates in WGS 84/UTM zone 32N (EPSG:32632).

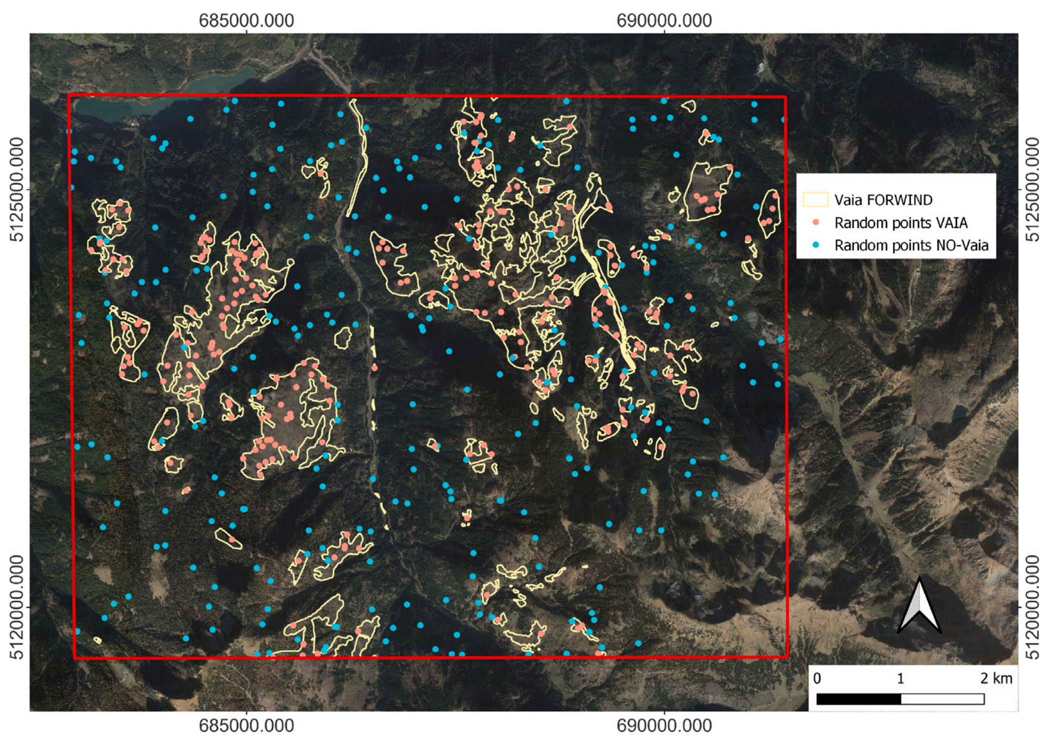

Fig. 2. In red, the border of one of the study area (Manghen study area). In yellow the FORWIND dataset indicating the forested area hit by the Vaia storm. In pink the random points within the FORWIND dataset and in blue the random points in the forested area not hit by the Vaia storm. Background image used: Google Image at February 20th 2024. Coordinates in WGS 84/UTM zone 32N (EPSG:32632).

Table 1
Geographic and forest cover data of the four study areas.

Study area	GPS center position (WGS 84 UTM 32N - EPSG: 32632)	Elevation range (m a.s.l.)	Forest area (ha)	% of forest area Hit by Vaia storm
Carezza	696 477.91, 5 143 104.94	From 1000 to 2800	3400	13.2%
Predazzo	702 596.13, 5 133 901.17	From 980 to 2400	3500	27.7%
Manghen	687 089.01, 5 122 828.43	From 700 to 2400	5100	14.3%
Primiero	719 328.66, 5 119 989.72	From 670 to 2300	4000	16.5%

by its rugged landscape, with altitudes that vary from around 670 m to 2300 m a.s.l..

In each study area, we randomly selected through the R (R Core Team, 2000) `spsample` function 250 square plots measuring 1 ha each (100 m × 100 m) within the regions affected by the Vaia storm, as well as another 250 plots of the same size within forested areas unaffected by the storm (Fig. 2).

2.2. FORWIND data-set

The FORWIND data-set (Forzieri et al., 2020), freely available here https://figshare.com/articles/dataset/A_spatially-explicit_database_of_wind_disturbances_in_European_forests_over_the_period_2000-2018/9555008 was used in this study to characterize the area hit by the Vaia windstorm (Figs. 1, 2). This dataset serves as a novel repository documenting wind disturbances in European forests. It encompasses over 80,000 spatially delineated areas across Europe that experienced wind-related disturbances between 2000 and 2018 (Forzieri et al., 2020). The information is presented in a standardized geographical vector format to ensure consistency. The dataset encompasses all significant windstorms recorded during the observational period, including the Vaia windstorm, making up approximately 30% of reported damaging wind events in Europe. To validate the reliability of FORWIND, correlation analyses with land cover changes derived from the Landsat-based Global Forest Change dataset and the MODIS Global Disturbance Index were conducted, affirming the robustness and accuracy of the FORWIND dataset (Forzieri et al., 2020). In addition to the validation performed by Forzieri et al. (2020), we conducted our own visual interpretation using high-resolution aerial images with a spatial resolution of 20 cm. For the Carezza study area, we used imagery from 2023 obtained from http://geokatalog.buergernetz.bz.it/geokatalog/#!, and for the Manghen, Predazzo, and Primiero study areas, we used imagery from 2020 available at https://webgis.provincia.tn.it/wgt/?lang=it&topic=1&catalogNodes=1,6&bgLayer=sfondo&layers=ammcom,orto2020&layers_visibility=false,true&X=5111866.50&Y=671432.76&zoom=5. Our visual interpretation revealed no inconsistencies between the FORWIND polygons and the observed wind damage in these areas.

2.3. LiDAR data

The LiDAR dataset for the Predazzo, Manghen and Primiero areas, collected through an ALS campaign in 2014, presented a point cloud density of approximately 15 points/m^2. In contrast, the Carezza dataset, collected by an ALS campaign in 2017, exhibited a lower density of around 1.5 points/m^2. Prior to further processing, the point cloud was classified into several categories including ground points, essential for generating different digital models used successively in our analysis. To ensure a standardized and comparable dataset for subsequent analysis, a uniform point cloud density of 1.5 points/m^2 was established for the Carezza area through the implementation of the `decimate_points` function within the `lidR` R package. This processing step was crucial for mitigating the potential influence of variations in point cloud density on the results, enabling a more robust and equitable comparison of the structural variables between the two regions.

2.4. Forest structural and topographic variables estimation

In our investigation, we centered our attention on three distinct structural forest variables that could be estimated through LiDAR data: HH, forest mean height, and forest density (Table 2). These variables were evaluated for each 1ha plot at both pixel and tree levels. At pixel level, LiDAR information was utilized through raster analysis, while at the tree level, the positions of individual trees within the study areas were extracted from LiDAR point cloud, and the corresponding variables were derived successively based on the identified trees.

At pixel level, the three structural variables were estimated using the Canopy Height Model (CHM). This was derived by normalizing the point clouds using the `tin` algorithm within the `lidR` R package. Subsequently, the CHM was generated using the `rasterize_canopy` function from the `lidR` package, implementing the `p2r()` algorithm. Prior to this, noise points were removed from the point cloud to ensure accuracy in the CHM, facilitating a more reliable representation of the structural variables. Striking a balance between spatial resolution and computational efficiency, and drawing insights from previous studies (Torresani et al., 2020; Tamburlin et al., 2021), we settled on a CHM spatial resolution of 2.5 m.

To estimate the structural variable at tree level (Table 2), individual trees (tree height and number of trees) were identified from the point cloud using the `locate_trees` function provided by the R `lidR` package.

2.4.1. Forest height heterogeneity

HH expresses the diversity in forest tree height derived from LiDAR data (e.g. from CHM) (Torresani et al., 2020). This measure, rooted in the Height Variation Hypothesis approach (analogous to the Spectral Variation Hypothesis that uses optical data Rocchini et al., 2017), states that increased HH correlates with heightened habitat heterogeneity and biodiversity. As demonstrated in various studies (Torresani et al., 2020, 2023b; Tamburlin et al., 2021), HH serves as an indicator of forest vertical structure, intricately linked to habitat diversity. The computation of HH entailed employing a heterogeneity index, which effectively measures the diversity within pixels. In this context, the HH in both areas affected and not affected by the Vaia storm was derived, for its proven effectiveness (Rocchini et al., 2017; Ricotta and Carranza, 2013; Ricotta and Marignani, 2007; Ricotta, 2005), using the Rao's Q index (Eq. (1)) at both pixel and tree level. The suitability of Rao's index for calculating different aspects of heterogeneity from remote sensing data had been previously validated in other studies (Perrone et al., 2024; Torresani et al., 2024a; Michele et al., 2018; Tamburlin et al., 2021; Torresani et al., 2024b). In contrast, its application for detecting HH at tree level was explored for the first time in this study. A review of the mathematical properties of this heterogeneity index is available in (Rocchini et al., 2024).

$$Q_{rs} = \sum_{i=1}^{F-1} \sum_{j=i+1}^{F} d_{ij} * p_i * p_j, \tag{1}$$

where:

Q_{rs} = Rao's Q index
p = relative abundance of a pixel value (at pixel level) or tree height (identified from the LiDAR point cloud using the R `locate_trees` function) value in a plot (F)
d_{ij} = distance between the ith and jth pixel value (at pixel level) or tree height (at tree level) value ($d_{ij} = d_{ji}$ and $d_{ii} = 0$)
i = pixel value (at pixel level)/tree height (at tree level) value i
j = pixel value (at pixel level)/tree height (at tree level) value j

The relative abundance p is calculated as the ratio between the considered pixel value or tree height value (p_i and p_j) and the total number of pixels/trees in F. As well discussed by Rocchini et al. (2017) the index allows to build a distance matrix d_{ij} in different dimensions, allowing the consideration of more than one band or raster at a time. In our case, and as used in different other studies (Torresani et al., 2020; Tamburlin et al., 2021), the d_{ij} was calculated as a simple Euclidean distance based on a single layer (CHM values or matrix of tree height values). The Rao's Q values were retrieved for each plots hit and not hit by the Vaia storm, implementing the R `spectralrao` function of the `rasterdiv` R package Rocchini et al. (2021).

2.4.2. Forest mean height

In each plot hit and not hit by the Vaia storm, the forest mean height was computed at pixel level, involving the calculation of the mean CHM values (Eq. (2)).

$$\text{Forest mean height}_{\text{pixel}} = \text{mean CHM} \tag{2}$$

where:

Forest mean height$_{\text{pixel}}$ = forest mean height computed at pixel level
mean CHM = mean of CHM values per plot

At tree-level it was determined by calculating the mean height of trees identified from the LiDAR point cloud (Eq. (3)).

$$\text{Forest mean height}_{\text{tree}} = \text{tree mean height} \tag{3}$$

where:

Forest mean height$_{\text{tree}}$ = tree mean height computed at tree level

Table 2
The table summarizes the structural variables used in this study (Forest Height Heterogeneity (HH), forest mean height and forest density) along with the corresponding dataset used for their derivation at pixel and tree level.

Structural variable	Dataset used at pixel level	Dataset used at tree level
Forest Height Heterogeneity (HH)	Canopy Height Model (CHM)	Height of trees detected from point cloud
Forest mean height	Canopy Height Model (CHM)	Height of trees detected from point cloud
Forest density	Canopy Height Model (CHM)	Number of trees detected through single tree detection from point cloud within a given area (1 ha)

tree mean height = the average height of each tree (within each plot), identified on the LiDAR point cloud by the R `locate_trees` function of the `lidr` R Package.

2.4.3. Forest density

Following the results of previous works (Torresani et al., 2020, 2023b), the forest density at pixel level was calculated as canopy cover for each plot hit and not hit by the Vaia storm through the following formula:

$$\text{Density}_{\text{pixel}} = \frac{px_{2\text{ m}}}{px_{\text{tot}}} \times 100 \tag{4}$$

where:

$Density_{pixel}$ = forest density estimated at pixel level
$\text{px}_{2\text{ m}}$ = number of pixels with a CHM > 2 m
px_{tot} = total number of pixels

The forest tree density at tree level was estimated as the number of trees per hectare, identified from the LiDAR point cloud using the `locate_trees` function of the `lidr` R Package.

$$\text{Density}_{\text{tree}} = \frac{N_{\text{trees}}}{1\text{ ha}} \tag{5}$$

where:

$\text{Density}_{\text{tree}}$ = forest density estimated at tree level
N trees = number of trees identified from the LiDAR point cloud using the R `locate_trees` function.

2.5. Topographic variables

In our investigation, we centered our attention also on three distinct topographic variables within the forest ecosystem: aspect, slope and altitude. These variables were assessed starting from the Digital Terrain Model (DTM) calculated from the LiDAR point cloud through the `tin()` algorithm within the `rasterize_terrain` function (`lidR` R Package). As for the CHM, the DTM was derived for all the study areas with a spatial resolution of 2.5 m.

Aspect and slope were estimated using the R `terrain` function, while the altitude was derived directly from the DTM. A final value of aspect, slope, and altitude for each plot hit and not hit by the Vaia storm were determined as the medians of the pixel values within each respective plot. Subsequently, the three variables were classified into distinct classes. For aspect classification, aspect values were categorized into nine predefined categories: North (ranging from 337.5° to 22.5°), North-East (ranging from 22.5° to 67.5°), East (ranging from 67.5° to 112.5°), South-East (ranging from 112.5° to 157.5°), South (ranging from 157.5° to 202.5°), South-West (ranging from 202.5° to 247.5°), West (ranging from 247.5° to 292.5°), North-West (ranging from 292.5° to 337.5°).

For slope classification, slope values were assigned to one of seven categories: Flat (ranging from 0° to 3°), Undulating (ranging from 3° to 8°), Moderately sloping (ranging from 8° to 15°), Hilly (ranging from 15° to 30°), Moderately steep (ranging from 30° to 45°), Steep (ranging from 45° to 65°), Very steep (for slopes greater than or equal to 65°), and Undefined (for slope values that do not fit into any defined range).

For altitude classification, altitude values were assigned to one of eight categories: less than 1000 m, 1000–1250 m, 1250–1500 m, 1500–1750 m, 1750–2000 m, 2000–2250 m, 2250–2500 m, and greater than or equal to 2500 m.

2.6. Statistical analysis

Structural variables such as forest height heterogeneity (HH), mean forest height, and forest density were calculated at both pixel and tree levels for areas affected and unaffected by the Vaia storm. Based on a normality assessment by the Shapiro–Wilk test, we found that some of the variables did not follow a normal distribution. Consequently, we opted to use the Wilcoxon test (two tailed - alpha level = 0.05) to compare these variables and evaluate the statistical significance of differences between the impacted and non-impacted plots. A similar approach was applied to the topographic characteristics, which were visualized using bar charts for comparison. Since the topographic data were categorized, allowing for class-based comparisons, a chi-square test (two tailed - alpha level = 0.05) was conducted to evaluate the association between slope, aspect, and altitude categories in Vaia-affected and unaffected plots.

A generalized linear mixed model (GLMM) regression analysis was applied to investigate the combined effects of topographic and structural characteristics on all the plots across the four study areas affected by the Vaia storm. GLMM was chosen because it is suitable for modeling the probability of an event occurring as a function of several predictors while accounting for the random effects of grouped data—in this case, the four study areas. This approach allowed us to account for potential non-independence of plots within the same region. The analysis included all the topographic (slope, aspect, altitude) and structural variables (forest density, forest HH, and forest mean height). We initially assessed multicollinearity among the predictors using the Variance Inflation Factor (through the `vif` function of the `car` R package) to ensure that no predictors were highly correlated. Following this, we constructed a series of models, beginning with a full model incorporating all main effects and potential interactions. Due to convergence issues and signs of overfitting in the initial models, we employed a stepwise model selection process to simplify the model by removing non-significant predictors and interactions, guided by AIC comparisons (using the `AIC` R function) and model convergence diagnostics. The final model included the effects of the forest structural variables, certain altitude ranges, and aspects, along with a random effect for the areas, providing a more parsimonious fit while capturing the key factors influencing the likelihood of damage. This approach allowed us to disentangle the influence of structural and topographical characteristics on storm damage more effectively, highlighting the complex interplay of these variables in our alpine forest ecosystems.

2.7. Workflow

The approach proposed in this study is summarized in Fig. 3. In each study area, we designated 250 random plots in both Vaia storm-impacted and unaffected forests. Pre-storm ALS LiDAR data was employed to evaluate structural attributes of the forest (before Vaia) such as HH, forest density, and forest mean height at both pixel and tree level. Topographic characteristics as slope, aspect and altitude were also derived from the LiDAR data. Different comparative analysis (Wilcoxon test, chi-square test and a generalized linear mixed model GLMM, to investigate the combined effects of structural and topographic characteristics on storm damage). The GLMM, which included random effects to account for the variability across the four study regions, allowed us to examine how these factors influenced the likelihood of a plot being affected by the Vaia storm. This comprehensive analysis provided insights into the complex interplay between forest structure, topography, and storm impact

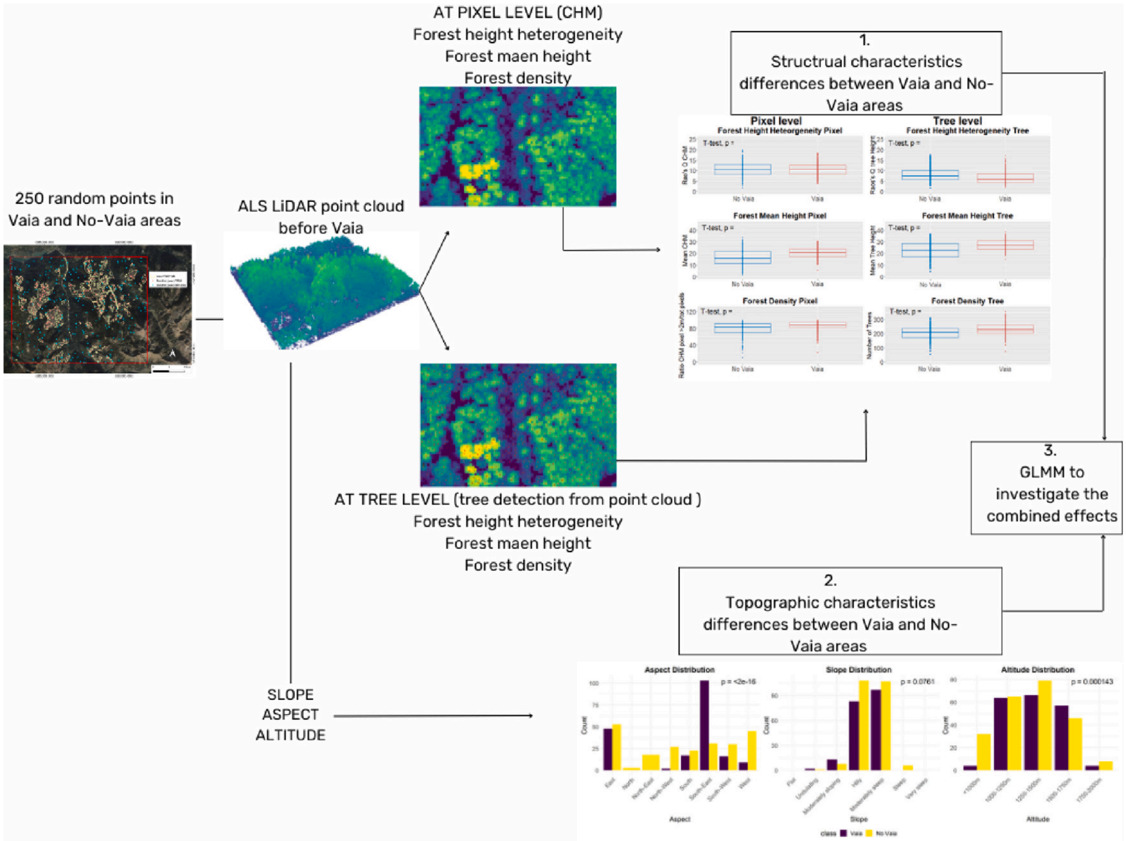

Fig. 3. For each study area, 250 random points were selected in regions affected and unaffected by the Vaia storm. ALS LiDAR data from before the storm were utilized to analyze structural forest characteristics, including forest height heterogeneity (HH), forest density, and forest mean height, at both pixel and tree levels. Additionally, topographic characteristics such as slope, aspect, and altitude were derived from the LiDAR point cloud. Statistical differences (Wilcoxon test, chi-square test and a GLMM in order to investigate the combined effect of structural and topographic characteristics) in structural and topographic characteristics between storm-affected and non-affected areas, were subsequently evaluated.

3. Results

The correlations among structural variables (forest HH, forest mean height, and forest density) assessed at both pixel and tree levels, comparing areas impacted and not impacted by the Vaia storm ("Vaia" and "No Vaia") in the Carezza, Predazzo, Manghen, and Primiero study areas are illustrated in Figs. 4, 5, 6, and 7, respectively.

Across all study areas, significant differences ($p < 0.05$, determined via Wilcoxon test) are observed in forest mean height in all the 4 study areas when evaluated at both pixel and tree levels. The results indicate that forest mean height is greater in the Vaia-affected forests compared to the unaffected regions. Forest density showed an unclear pattern, at pixel and tree level it shows significant differences in Manghen and in Predazzo while it was not in the other 2 study areas. Finally forest HH, estimated at pixel and tree level, does not exhibit significant differences (Wilcoxon test > 0.05), between the two types of areas in all locations (except in Manghen and Predazzo study area when the analysis were conducted at tree level).

The topographic characteristics of the "Vaia" and "No Vaia" areas, for the Carezza, Predazzo, Manghen and Primiero study areas are shown in Figs. 8–11 respectively. The analysis revealed significant differences in aspect, slope, and altitude between "Vaia" and "No Vaia" areas.

Aspect exhibited notable and significant variations between storm-hit and unaffected areas in all the 4 areas. In Manghen study area, "Vaia" plots predominantly faced East, while in Predazzo study area, they displayed a varied distribution with a notable presence of South-East directions. Primiero study area showed similar variations, with higher frequencies of South-East directions observed in "Vaia" plots. Carezza exhibited diverse aspect distributions, with "Vaia" plots facing North-East and South-East.

Altitude also displayed notable and significant variations between storm-hit and non-unaffected areas as well in the 4 study areas. "Vaia" plots had in general higher frequencies in middle altitude categories.

Slope exhibited significant differences between storm-affected and unaffected regions, although to a lesser extent when compared to altitude and aspect (in Carezza study area the difference was not significant). In Manghen study area, "Vaia" plots displayed higher frequencies of Hilly and Moderately steep terrains compared to "No Vaia" plots. These trends were consistent across other study areas, including Predazzo, Primiero and Carezza study area.

The output of the GLMM analysis at both pixel and tree level, which included both structural and topographical variables, revealed several key predictors of Vaia storm damage across the study plots. Before finalizing the models, we assessed multicollinearity among the predictors using the VIF, ensuring that collinearity was not a concern. We then proceeded with a stepwise model selection, guided by AIC and significance testing, to simplify the model while retaining the key predictors. Interaction terms were explored but were ultimately excluded from the final model due to convergence issues and overfitting concerns, which indicated that simpler models provided more reliable and interpretable results. After the reduction, we arrived at the two final models (one for the pixel and one for the tree analysis), which best captures the factors influencing storm impact. Details of the other models tested during the selection process can be found in the Supplementary material (Analysis at pixel level - Analysis at tree level).

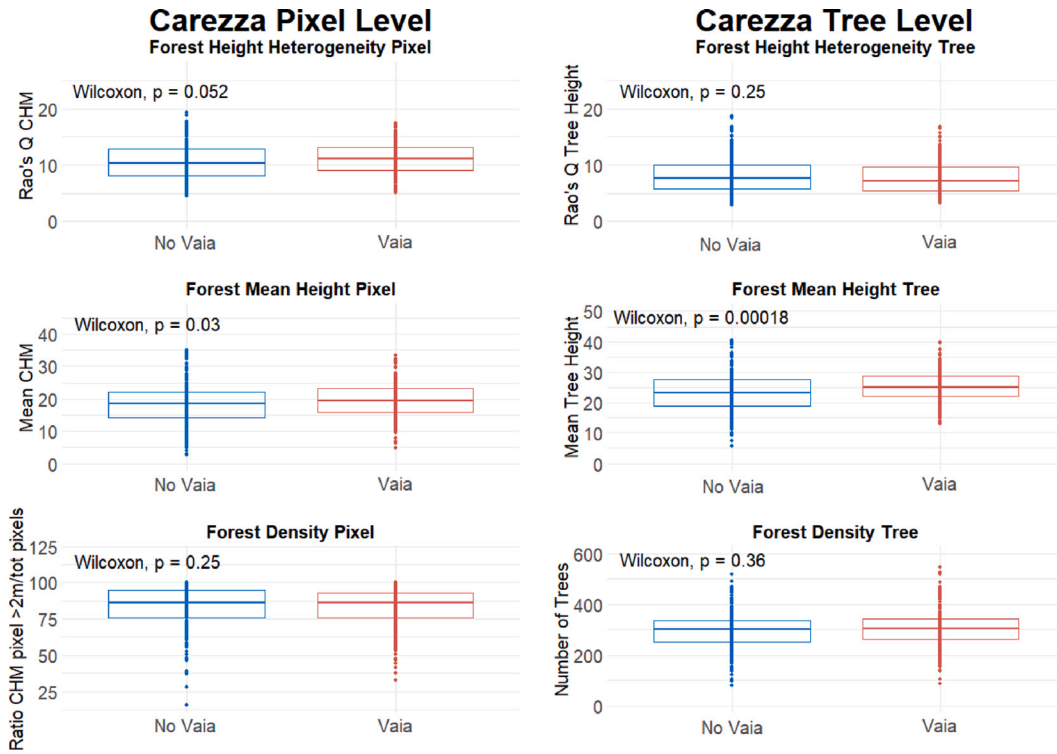

Fig. 4. The figure shows the correlation of the structural variables (forest HH, forest mean height and forest density) assessed at pixel and tree level, between "Vaia" and "No Vaia" areas of Carezza.

Fig. 5. The figure shows the correlation of the structural variables (forest HH, forest mean height and forest density) assessed at pixel and tree level, between "Vaia" and "No Vaia" areas of Predazzo.

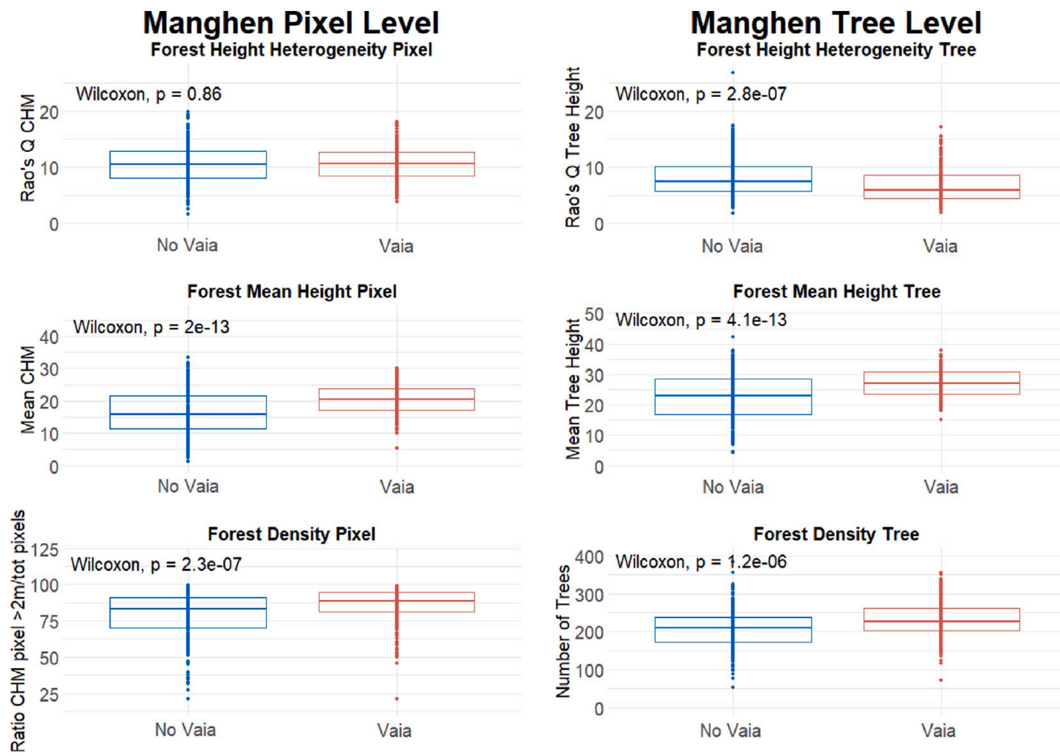

Fig. 6. The figure shows the correlation of the structural variables (forest HH, forest mean height and forest density) assessed at pixel and tree level, between "Vaia" and "No Vaia" areas of Manghen.

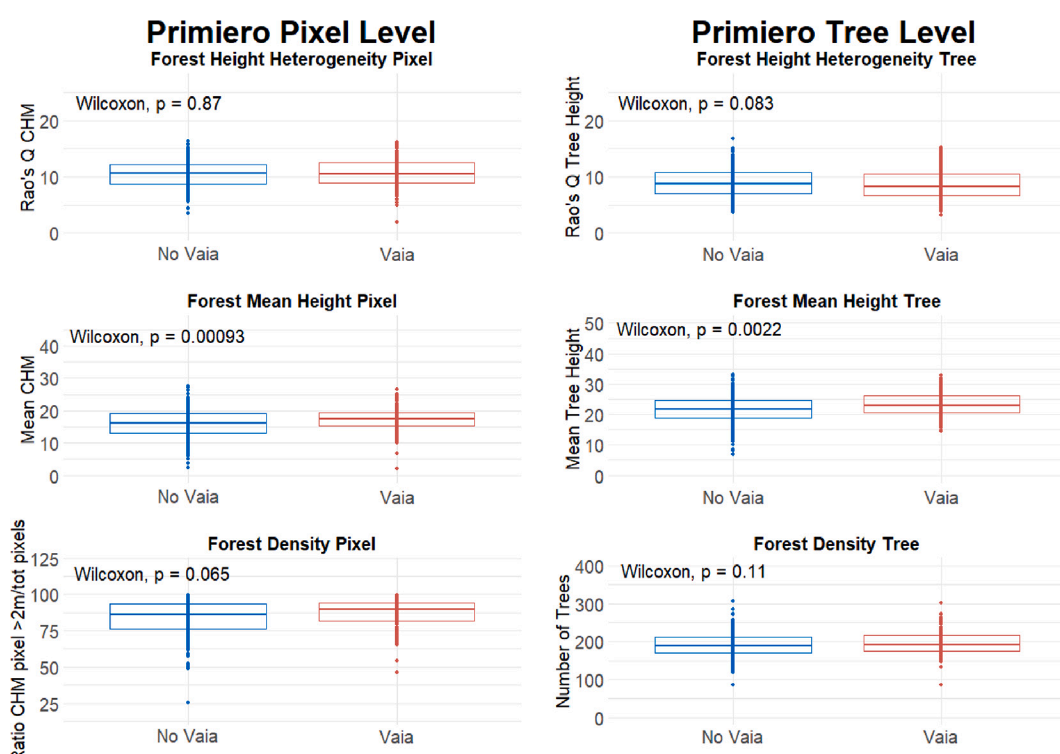

Fig. 7. The figure shows the correlation of the structural variables (forest HH, forest mean height and forest density) assessed at pixel and tree level, between "Vaia" and "No Vaia" areas of Primiero.

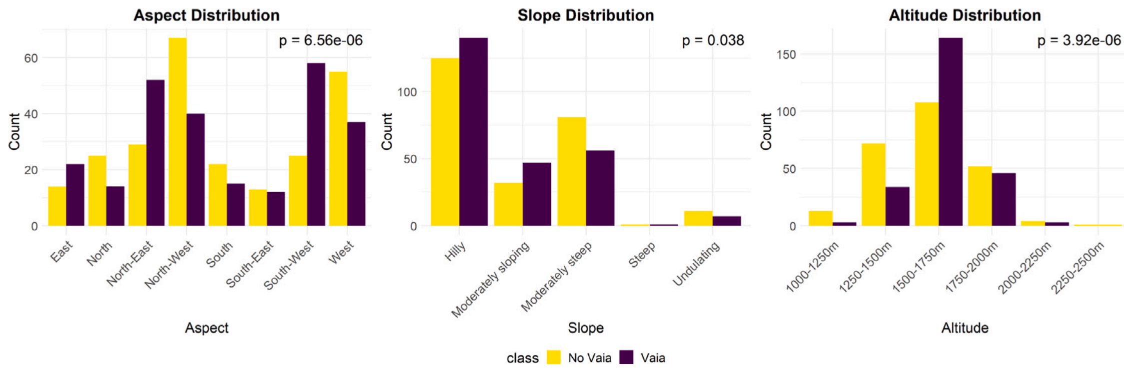

Fig. 8. Difference in aspect, slope and altitude of the plots in "Vaia" and "No Vaia" areas in the Carezza study area. P value is referred to chi-square test.

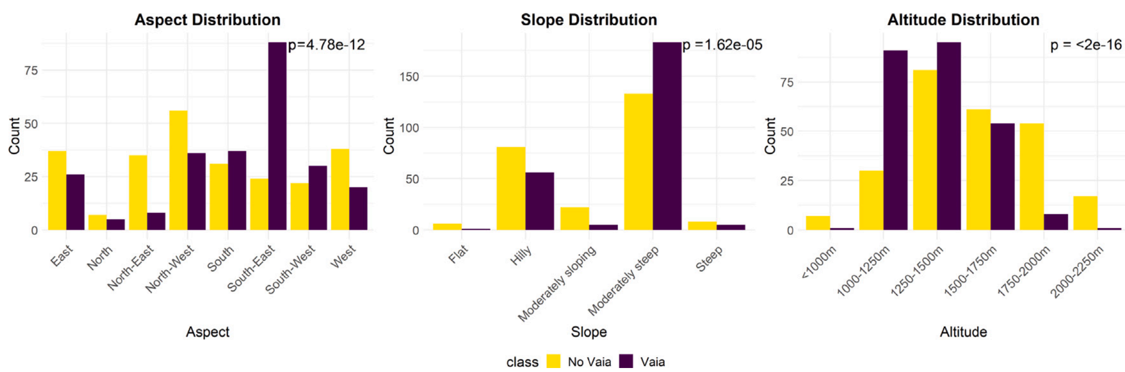

Fig. 9. Difference in aspect, slope and altitude of the plots in "Vaia" and "No Vaia" areas in the Predazzo study area. P value is referred to chi-square test.

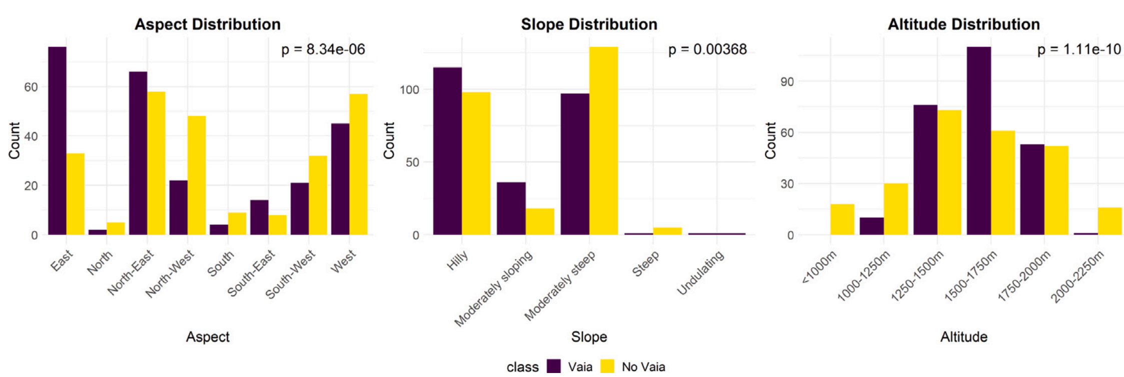

Fig. 10. Difference in aspect, slope and altitude of the plots in "Vaia" and "No Vaia" areas in the Manghen study area. P value is referred to chi-square test.

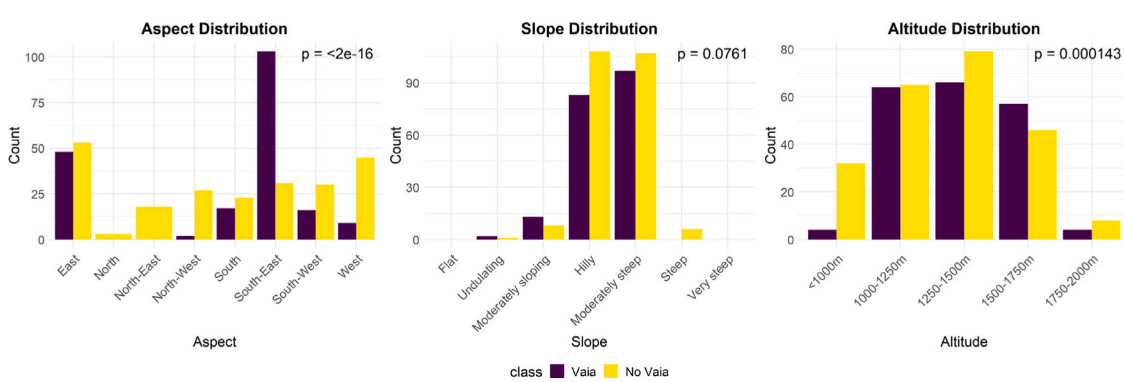

Fig. 11. Difference in aspect, slope and altitude of the plots in "Vaia" and "No Vaia" areas in the Primiero study area. P value is referred to chi-square test.

Table 3
Generalized Linear Mixed Model (GLMM) results for the analysis at pixel level predicting the likelihood of storm impact based on topographic and structural variables, after a stepwise model selection process.

Variable	Estimate	Std. Error	z value	p-value
(Intercept)	−4.3655	0.7910	−5.519	3.40×10^{-8} ***
Forest height heterogeneity (HH) at pixel level	0.0401	0.0218	1.838	0.0660 .
Forest mean height	0.0843	0.0149	5.656	1.55×10^{-8} ***
Forest density	0.0041	0.0063	0.650	0.5154
altitude1000–1250 m	2.4694	0.5465	4.518	6.23×10^{-6} ***
altitude1250–1500 m	2.2714	0.5405	4.202	2.64×10^{-5} ***
altitude1500–1750 m	2.8261	0.5414	5.220	1.79×10^{-7} ***
altitude1750–2000 m	2.4067	0.5528	4.354	1.34×10^{-5} ***
altitude2000–2250 m	1.3753	0.7492	1.836	0.0664 .
altitude2250–2500 m	−7.7935	462.1884	−0.017	0.9865
aspectNorth	−1.4553	0.3174	−4.585	4.54×10^{-6} ***
aspectNorth-East	−0.7743	0.1849	−4.189	2.81×10^{-5} ***
aspectNorth-West	−1.2887	0.1851	−6.963	3.33×10^{-12} ***
aspectSouth	−0.2952	0.2134	−1.383	0.1666
aspectSouth-East	1.0617	0.1935	5.485	4.13×10^{-8} ***
aspectSouth-West	−0.1539	0.1893	−0.813	0.4163
aspectWest	−0.9035	0.1786	−5.060	4.19×10^{-7} ***

Signif. codes: 0 '***' 0.001 '**' 0.01 '*' 0.05 '.' 0.1 ' ' 1.

Table 4
Generalized Linear Mixed Model (GLMM) results for the analysis at tree level predicting the likelihood of storm impact based on topographic and structural variables, after a stepwise model selection process.

Variable	Estimate	Std. Error	z value	p-value
(Intercept)	−5.268	0.6989	−7.538	4.77×10^{-14} ***
Forest height heterogeneity (HH) at tree level	0.0007932	0.01868	0.042	0.9661
Forest mean height	0.09053	0.01004	9.021	$<2 \times 10^{-16}$ ***
Forest density	0.00441	0.0008471	5.206	1.93×10^{-7} ***
altitude1000–1250 m	2.417	0.5486	4.405	1.06×10^{-5} ***
altitude1250–1500 m	2.184	0.5427	4.025	5.70×10^{-5} ***
altitude1500–1750 m	2.676	0.5435	4.924	8.48×10^{-7} ***
altitude1750–2000 m	2.329	0.5552	4.196	2.72×10^{-5} ***
altitude2000–2250 m	1.397	0.7488	1.865	0.0621 .
altitude2250–2500 m	−10.04	77.19	−0.130	0.8965
aspectNorth	−1.587	0.3187	−4.980	6.35×10^{-7} ***
aspectNorth-East	−0.8036	0.1879	−4.277	1.89×10^{-5} ***
aspectNorth-West	−1.349	0.1868	−7.219	5.25×10^{-13} ***
aspectSouth	−0.2505	0.2154	−1.163	0.2449
aspectSouth-East	1.079	0.1975	5.463	4.68×10^{-8} ***
aspectSouth-West	−0.1286	0.1899	−0.677	0.4983
aspectWest	−0.8978	0.1800	−4.987	6.14×10^{-7} ***

Signif. codes: 0 '***' 0.001 '**' 0.01 '*' 0.05 '.' 0.1 ' ' 1.

In the GLMM analysis at the pixel level (Table 3), forest mean height emerged as a significant predictor, with a positive correlation indicating that areas with taller vegetation were more likely to experience damage. Aspect also played a crucial role in storm impact, with the 'South-East' aspect showing a significant positive association with the likelihood of damage. In contrast, 'North', 'North-East', and 'North-West' aspects were associated with a decreased likelihood of being affected. Altitude was another significant factor, with specific elevation ranges, particularly between 1000–2000 m, showing an increased likelihood of storm impact. However, the highest altitude category (2250–2500 m) did not show a significant influence, implying that storm susceptibility might decrease at these extreme elevations.

Similar results were obtained in the GLMM analysis at the tree level (Table 4). Forest mean height once again emerged as a significant predictor, similar to the pixel-level analysis. A positive correlation was observed, indicating that trees in areas with taller vegetation were more likely to experience damage during the storm. However, unlike the pixel-level analysis, forest density showed a significant positive effect in this final model. In terms of aspect, both analyses identified 'South-East' as having a significant positive association with damage likelihood, suggesting that this aspect consistently increases storm susceptibility across scales. Altitude remained a significant factor in the tree-level analysis as well, with similar patterns as observed in the per pixel analysis: the 1000–2000 m range showed an increased likelihood of storm impact, while the highest category (2250–2500 m) was not significant.

4. Discussion

In this study, we explored the influence of forest structural variables (including forest height heterogeneity, mean height, and tree density) alongside topographic factors (such as aspect, slope, and altitude) estimated from LiDAR data, on the extent of damage caused by the Vaia windstorm, offering valuable insights into the dynamics of forest vulnerability to extreme wind events. Our findings, derived from both applied methodologies (at the pixel and tree levels), indicate that in cases of forest wind damage, forest mean height tends to be higher in areas affected by the windstorm, compared to unaffected ones. Forest density also plays a lesser but important role, with denser areas experiencing more severe damage than less dense areas, though this was only significant in certain areas. This seemingly indicates that conifer forests (typical of the study areas) with taller and denser tree populations are more vulnerable to wind damage due to their increased exposure and mechanical leverage against strong wind forces. Additionally, these trees might have a higher height to diameter at breast height (DBH) ratio, leading to a structurally weaker form, akin to being overly thin, which decreases their stability against wind. This structural weakness is compounded by the fact that denser forests might be more susceptible to various environmental stressors, including water stress (Bottero et al., 2017), potentially predisposing these stands to disturbances like those experienced during the Vaia windstorm. Furthermore, such regions may experience enhanced vulnerability due to a "domino effect", where the damage is amplified as falling trees trigger further tree falls. These findings are in partial agreement with existing studies, Albrecht et al. (2012) and Mitchell (2013) have both highlighted the role of structure variables in determining wind damage susceptibility, with taller trees generally facing higher risk and dense forests that could explain storm damage.

Interestingly, forest HH, estimated at pixel and tree level, did not show a significant difference between affected and unaffected areas. This deny the initial hypothesis that higher HH, indicative of a more diverse vertical structure, would contribute to increased windthrow resistance. This phenomenon may be due to the forests' adaptive characteristics or resilience, where structural uniformity across different areas has evolved to mitigate the impact of wind events. It could also indicate that the inherent structural stability of these forests, possibly due to lower canopy profiles or uniform root systems, provides natural resistance against strong winds. Additionally, microclimatic conditions or topographical features specific to these locations might play a crucial role in reducing wind impact. Methodological considerations in assessing HH and its impact on forest resilience might not capture all nuances, suggesting a need for further research into other factors like species diversity and spatial arrangement.

The GLMM results furthermore emphasized that specific aspects significantly influenced the likelihood of the area being impacted by the Vaia storm. In particular, 'North', 'North-East', 'North-West', and 'West' aspects were associated with a lower risk, indicating a negative influence. Conversely, the 'South-East' aspect demonstrated a positive influence, suggesting a higher likelihood of storm impact. This aligns with findings by Giovannini et al. (2021) and Olmo et al. (2021), who reported that during the Vaia storm, a deep low-pressure system developed over the Mediterranean, generating strong southerly winds that struck the eastern Italian Alps. Meteorological stations across the region recorded wind gusts exceeding 50 m/s, primarily driven by a powerful southerly low-level jet that intensified ahead of an approaching cold front.

As previously stressed, it is essential to approach these results with caution due to various influencing factors on forest mean height and density, including altitude. As the analysis was conducted in a mountainous area, where Vaia had the most impact, it is well-established that tree height and density decreases with higher altitudes. To account for this, when comparing areas affected and unaffected by Vaia, the selection of both affected and unaffected forested areas was randomized. This random selection could include unaffected forested areas at the top of the vegetation belt, where tree height and density tends to be lower. For this reason, we conducted further analysis using a GLMM model to precisely understand the impact of structural and topographic variables on storm damage and to understand the conditions under which forests are more susceptible to storm damage. These analyses enhanced our understanding of the topographic and structural factors contributing to storm susceptibility in forest areas, aiding in the prediction and assessment of risk factors for future storm events.

4.1. Forest management

Various studies have pointed out the significant role of forest management in reducing the impacts of wind on forests. Specifically, modifying thinning practices to decrease forest density may be considered and potentially recommended as a means to enhance the resilience of forests against windstorms, especially in areas frequently hit by such extreme weather events (Albrecht et al., 2012). However, it is crucial to note that the immense scale of the Vaia windstorm was the primary and most forceful factor leading to the widespread damage observed, underscoring the dominant influence of the extreme weather event itself. The Vaia windstorm was exceptionally powerful, with wind speeds reaching up to 180 km/h (Giovannini et al., 2021). Additionally, it triggered an extraordinary amount of rainfall, with some regions receiving up to 850 mm in just three days (Giovannini et al., 2021; Lucianetti et al., 2019; Davolio et al., 2023) compared to the typical annual rainfall of approximately 1200 mm. Moreover, topographical analyses indicated that the storm's impact was not uniform across different terrains; the wind penetrated valleys and affected various parts of the mountains, each with distinct altitudes, slopes, and orientations. This variability makes it challenging to devise adaptive management strategies that consider the complex interactions between forest structure, topography, and the impact of storms. Generally speaking, although diverse vertical structures may not necessarily improve forest resistance to windstorms, managing stand structure through density management can be critical to windstorm resilience following extreme events. Stand density affects the overall health of trees, not only the structure and growth of forests, in turn their functions.

4.2. Importance of remote sensing and of the used methodology

The study highlights the potential of remote sensing technologies, particularly LiDAR, in improving our understanding of forest structure and dynamics. LiDAR data provide valuable three-dimensional information and efficiently cover large areas, making them a practical, time-efficient option for assessing large-scale natural events like forest disturbances, especially in difficult-to-access regions (Huang et al., 2013; Ahmed et al., 2014). LiDAR data have also been employed in various related areas, such as in models predicting wind damage (Costa et al., 2023), estimating biomass loss after windstorms (Vaglio Laurin et al., 2021) or monitoring post-disturbance forest recovery (Senf et al., 2019). However, LiDAR has limitations in terms of spatial and temporal resolution, and its role should be seen as complementary to traditional field methods.

The methodology employed for estimating structural variables in our study represented just one viable approach. We opted for a dual analysis, performing at pixel and tree level to uncover potential disparities and similarities in forest structural variables using LiDAR data. Each approach has its distinct advantages and limitations. The per pixel approach utilizes the CHM in a raster format, providing a broad overview of forest structure over large areas efficiently and economically. This method excels at capturing spatial patterns across extensive regions, making it ideal for large-scale analysis. However, it may lack the precision needed to detail individual tree characteristics, which could lead to generalizations in forest density and height heterogeneity estimates. In contrast, the per tree analysis extracts individual tree data from LiDAR point clouds, offering greater precision in assessing forest composition and structural diversity, especially at a smaller scale. This method provides detailed, tree-level insights but can be more computationally intensive and less reliable in areas with dense canopies, where accurately detecting individual trees is challenging. Furthermore this approach is limited by its reliance on specific algorithms, which reduces its effectiveness across large forest landscapes. By employing both approaches, we aimed to complement the large-scale efficiency of per pixel analysis with the fine-scale precision of per tree analysis.

For HH estimation, we chose Rao's Q index as the heterogeneity metric, a choice supported by its proven efficacy in various studies (Tamburlin et al., 2021; Torresani et al., 2020, 2023b), including applications in Spectral Variation Hypothesis studies (Torresani et al., 2024b; Rocchini et al., 2017; Thouverai et al., 2022; Perrone et al., 2024). This index, integrating both relative abundance and pixel values through Euclidean distance, encapsulates the entire structural information derived from LiDAR data heterogeneity (Torresani et al., 2022). When employed with a single layer or raster, as in our study with CHM at pixel level and tree height at tree level, Rao's Q effectively serves as a robust proxy for heterogeneity, converging to variance using half the squared Euclidean distance ($1/2\ d_{ij}^2$).

At pixel level, we opted to utilize the CHM as the initial variable for HH assessment, neglecting other LiDAR metrics pertinent to forest structure. This choice is substantiated by the findings of Tamburlin et al. (2021), where a comprehensive exploration of various LiDAR metrics (such as entropy, standard deviation of point cloud distribution, and percentage of returns above mean height) was conducted for HH estimation. The results of their study revealed that the CHM emerged as the most effective metric for characterizing HH and tree species diversity. The estimation of HH was firstly done applying the concept of the Height Variation Hypothesis, an indirect approach used to estimate forest biodiversity through remote sensing data stating that greater tree HH measured by CHM LiDAR data indicates higher forest structure complexity and tree species diversity. This concept has been tested using airborne (Torresani et al., 2020; Tamburlin et al., 2021) and Spaceborne (from the GEDI sensor Torresani et al., 2023b) LiDAR data showing good results.

4.3. Ecological aspect

It is worth mentioning that, a part of our results, we recognize the multifaceted nature of windthrow as not solely catastrophic events but as integral components of forest dynamics. Different studies (Mitchell, 2013; Jactel et al., 2017) elucidate that windthrow should be regarded as a recurring ecological process, contributing to the shaping of forest structures, influencing soil processes, and altering landscape patterns over time. This perspective is critical when considering the differential impacts observed in our study, where the structural variables of forest mean height and density, alongside topographic elements, played significant roles in determining the susceptibility of areas to the Vaia windstorm (Mitchell, 2013). It is necessity of considering the long-term ecological consequences of windthrow, including its effects on stand dynamics and soil properties. This underlines the complexity of interactions between tree, weather, and site conditions, which are crucial for understanding and predicting windthrow patterns and impacts. The role of soil conditions and terrain features, as discussed by Mitchell (2013), in affecting local stand vulnerability offers a deeper understanding of the observed variability in storm damage across different forested landscapes in our study.

4.4. Limitations

Acknowledging the potential limitations of our research is crucial. While our focus was on the impact of forest structure and topography on wind damage caused by the Vaia storm, we recognize that other factors such as soil proprieties, stand age, percentage of conifers and recent thinning or edge exposure by harvesting also significantly influence wind damage outcomes, as highlighted in prior studies (Dobbertin, 2002; Mitchell, 2013; Valinger et al., 2000; Jactel et al., 2017). Our primary goal was to explore the feasibility of using LiDAR data to investigate the roles of structural and topographic factors in windstorm damages. To our knowledge, this is the first time such data have been applied in this context, marking an initial step toward understanding these dynamics. Moreover, the methodology we employed could present additional limitations. We chose to analyze random points within areas rather than encompassing all areas, acknowledging the disparity in size between the region impacted by the Vaia storm and the broader forested areas not affected. This choice was made to ensure a statistically robust comparison of similarly sized areas. Moreover, the characteristics of the LiDAR data, including its spatial resolution and the algorithms utilized for data processing, may introduce certain limitations to the analysis. Also the time lag between when the LiDAR data was collected and the occurrence of the Vaia windstorm, which varies from two to four years across the research locations, is another potential drawback. While this temporal discrepancy is not optimal, it is a typical issue in studies that depend on LiDAR data, which often is not updated regularly due to the infrequent scheduling of LiDAR surveying campaigns (Polychronaki et al., 2015; Moudrỳ et al., 2021; Torresani et al., 2020). Despite this, we are confident that this temporal mismatch does not detract from the validity of our conclusions.

The results highlight a crucial need for proactive anticipation and preparation for unprecedented extreme events, particularly in the face of escalating climate change. Rather than focusing solely on forest management strategies, the integration of knowledge of ecological processes, the long-term impacts of windthrow on ecosystem dynamics and a shift toward addressing the root cause—climate change. This emphasizes the importance of changing our habits and collectively working to mitigate climate change, which is the primary driver of intensified disturbances. Beyond the immediate study context, a global call for preparedness urges a comprehensive reassessment of environmental policies and resource allocation to effectively tackle the evolving landscape of ecological threats, safeguarding the long-term sustainability of our forests.

5. Conclusion

This research showed how forest structure and topography influence storm damage vulnerability, in particular in area affected by the Vaia storm. Utilizing ALS LiDAR data, we have identified that taller and denser forests are more susceptible to wind damage, likely due to increased mechanical leverage against strong winds and possible structural weaknesses. Our findings align partially with previous research but also present unique insights, particularly concerning forest HH, which did not correlate with increased wind resistance as expected. Additionally, the role of altitude, slope and aspect in affecting forest structure and density was significant, necessitating the application GLMM to accurately assess these effects devoid of topographic-related confounding factors. This comprehensive approach highlights the complex interactions between natural forest dynamics and extreme weather events.

It is worth underlying that, while Vaia was a particularly severe event, the same methods used in this study can be applied to smaller, more frequent wind disturbances. By detecting subtle changes in forest structure and topography, these tools allow for improved preparedness and mitigation strategies, even in the case of lower-intensity events. This broadens the potential application of our study, providing value for ongoing forest management practices in regions prone to wind damage.

Future research should delve deeper into the relationships between forest structure and wind damage by incorporating more comprehensive datasets that include continuous monitoring before and after storm events. This could involve integrating other remote sensing technologies like satellite imagery or drone surveillance to enhance the spatial and temporal resolution of data. Studies could also explore the impact of biodiversity on resilience to wind damage, examining how different species compositions and forest management practices influence susceptibility providing valuable insights for policy and conservation efforts.

CRediT authorship contribution statement

Michele Torresani: Writing – review & editing, Writing – original draft, Validation, Methodology, Investigation, Formal analysis, Data curation, Conceptualization. **Leonardo Montagnani:** Conceptualization. **Duccio Rocchini:** Writing – review & editing, Methodology, Investigation, Conceptualization. **Vítězslav Moudrý:** Writing – review & editing, Validation, Methodology, Formal analysis, Conceptualization. **Andrea Andreoli:** Conceptualization. **Camilla Wellstein:** Writing – review & editing, Methodology, Conceptualization. **Kenta Koyanagi:** Writing – review & editing, Investigation, Formal analysis, Conceptualization. **Luca Da Ros:** Writing – review & editing, Investigation, Conceptualization. **Giovanni Bacaro:** Data curation, Conceptualization. **Michela Perrone:** Writing – review & editing, Methodology, Investigation, Conceptualization. **Chiara Salvatori:** Writing – review & editing, Visualization, Conceptualization. **Irene Menegaldo:** Writing – review & editing, Visualization, Conceptualization. **Enrico Guatelli:** Visualization, Conceptualization. **Roberto Tognetti:** Writing – review & editing, Supervision, Investigation, Funding acquisition, Formal analysis, Conceptualization.

Declaration of competing interest

The authors declare that they have no known competing financial interests or personal relationships that could have appeared to influence the work reported in this paper.

Appendix A. Supplementary data

Supplementary material related to this article can be found online at https://doi.org/10.1016/j.agrformet.2024.110267.

Data availability

The used data are open-source.

References

Abram, N.J., Henley, B.J., Sen Gupta, A., Lippmann, T.J., Clarke, H., Dowdy, A.J., Sharples, J.J., Nolan, R.H., Zhang, T., Wooster, M.J., et al., 2021. Connections of climate change and variability to large and extreme forest fires in southeast Australia. Commun. Earth Environ. 2 (1), 8.

Ahmed, O.S., Franklin, S.E., Wulder, M.A., 2014. Interpretation of forest disturbance using a time series of landsat imagery and canopy structure from airborne lidar. Can. J. Remote Sens. 39 (6), 521–542.

Albrecht, A., Hanewinkel, M., Bauhus, J., Kohnle, U., 2012. How does silviculture affect storm damage in forests of south-western Germany? Results from empirical modeling based on long-term observations. Eur. J. Forest Res. 131 (1), 229–247.

Béland, M., Kobayashi, H., 2021. Mapping forest leaf area density from multiview terrestrial lidar. Methods Ecol. Evol. 12 (4), 619–633.

Borrelli, P., Panagos, P., Märker, M., Modugno, S., Schütt, B., 2017. Assessment of the impacts of clear-cutting on soil loss by water erosion in Italian forests: First comprehensive monitoring and modelling approach. Catena 149, 770–781.

Bottero, A., D'Amato, A.W., Palik, B.J., Bradford, J.B., Fraver, S., Battaglia, M.A., Asherin, L.A., 2017. Density-dependent vulnerability of forest ecosystems to drought. J. Appl. Ecol. 54 (6), 1605–1614.

Costa, M., Gardiner, B., Locatelli, T., Marchi, L., Marchi, N., Lingua, E., 2023. Evaluating wind damage vulnerability in the alps: A new wind risk model parametrisation. Agricult. Forest. Meterol. 341, 109660.

Davolio, S., Vercellino, M., Miglietta, M.M., Pitura, L.D., Laviola, S., Levizzani, V., 2023. The influence of an atmospheric river on a heavy precipitation event over the western alps. Weather Clim. Extrem. 39, 100542.

Dobbertin, M., 2002. Influence of stand structure and site factors on wind damage comparing the storms Vivian and Lothar. Snow Landsc. Res. 77 (1/2), 187–205.

Domingo, D., Pérez-Rodríguez, F., Gómez-García, E., Rodríguez-Puerta, F., 2023. Assessing the efficacy of phenological spectral differences to detect invasive alien Acacia dealbata using sentinel-2 data in Southern Europe. Remote Sens. 15 (3), 722.

Du, L., Pang, Y., Wang, Q., Huang, C., Bai, Y., Chen, D., Lu, W., Kong, D., 2023. A LiDAR biomass index-based approach for tree-and plot-level biomass mapping over forest farms using 3D point clouds. Remote Sens. Environ. 290, 113543.

European Environment Agency, 2017. Climate Change Adaptation and Disaster Risk Reduction in Europe: Enhancing Coherence of the Knowledge Base, Policies and Practices. Office for Official Publ. of the Europ. Communities.

Forzieri, G., Pecchi, M., Girardello, M., Mauri, A., Klaus, M., Nikolov, C., Rüetschi, M., Gardiner, B., Tomaštík, J., Small, D., et al., 2020. A spatially explicit database of wind disturbances in European forests over the period 2000–2018. Earth Syst. Sci. Data 12 (1), 257–276.

Gamze, Ö., Çorumluoğlu, Ö., 2023. Assessment of forest fire damage severity by remote sensing techniques. Int. J. Environ. Geoinform. 10 (2), 151–158.

Giannetti, F., Pecchi, M., Travaglini, D., Francini, S., D'Amico, G., Vangi, E., Cocozza, C., Chirici, G., 2021. Estimating VAIA windstorm damaged forest area in Italy using time series sentinel-2 imagery and continuous change detection algorithms. Forests 12 (6), 680.

Giannetti, F., Travaglini, D., Nocentini, S., Francini, S., D'Amico, G., Calvo, E., Fasolini, D., Broll, M., Maistrelli, F., et al., 2019. Stima dei danni della tempesta "Vaia" alle foreste in Italia. Forest 16, 3–9.

Giovannini, L., Davolio, S., Zaramella, M., Zardi, D., Borga, M., 2021. Multi-model convection-resolving simulations of the october 2018 Vaia storm over northeastern Italy. Atmos. Res. 253, 105455.

Huang, W., Sun, G., Dubayah, R., Cook, B., Montesano, P., Ni, W., Zhang, Z., 2013. Mapping biomass change after forest disturbance: Applying LiDAR footprint-derived models at key map scales. Remote Sens. Environ. 134, 319–332.

Jactel, H., Bauhus, J., Boberg, J., Bonal, D., Castagneyrol, B., Gardiner, B., Gonzalez-Olabarria, J.R., Koricheva, J., Meurisse, N., Brockerhoff, E.G., 2017. Tree diversity drives forest stand resistance to natural disturbances. Curr. For. Rep. 3, 223–243.

Kamp, J., Trappe, J., Dübbers, L., Funke, S., 2020. Impacts of windstorm-induced forest loss and variable reforestation on bird communities. Forest Ecol. Manag. 478, 118504.

Kuzu, R.S., Antropov, O., Molinier, M., Dumitru, C.O., Saha, S., Zhu, X.X., 2024. Forest disturbance detection via self-supervised and transfer learning with sentinel-1&2 images. IEEE J. Sel. Top. Appl. Earth Obs. Remote Sens..

Le, T.S., Harper, R., Dell, B., 2023. Application of remote sensing in detecting and monitoring water stress in forests. Remote Sens. 15 (13), 3360.

Lucianetti, G., Mastrorillo, L., Mazza, R., Partel, P., 2019. Groundwater response to precipitation extremes: the case of the" vaia" storm (eastern Italian alps). Acque Sotterranee-Italian J. Groundw. 8 (4).

Marvasti-Zadeh, S.M., Goodsman, D., Ray, N., Erbilgin, N., 2023. Early detection of bark beetle attack using remote sensing and machine learning: A review. ACM Comput. Surv. 56 (4), 1–40.

McKenna, P.B., Lechner, A.M., Hernandez Santin, L., Phinn, S., Erskine, P.D., 2023. Measuring and monitoring restored ecosystems: can remote sensing be applied to the ecological recovery wheel to inform restoration success? Restor. Ecol. 31 (1), e13724.

Michele, T., Duccio, R., Marc, Z., Ruth, S., Giustino, T., 2018. Testing the spectral variation hypothesis by using the RAO-Q index to estimate forest biodiversity: Effect of spatial resolution. In: IGARSS 2018-2018 IEEE International Geoscience and Remote Sensing Symposium. IEEE, pp. 1183–1186.

Mitchell, S., 2013. Wind as a natural disturbance agent in forests: a synthesis. Forestry 86 (2), 147–157.

Moudrỳ, V., Bazzichetto, M., Remelgado, R., Devillers, R., Lenoir, J., Mateo, R.G., Lembrechts, J.J., Sillero, N., Lecours, V., Cord, A.F., et al., 2024. Optimising occurrence data in species distribution models: sample size, positional uncertainty, and sampling bias matter. Ecography e07294.

Moudrỳ, V., Moudrá, L., Barták, V., Bejček, V., Gdulová, K., Hendrychová, M., Moravec, D., Musil, P., Rocchini, D., Šťastnỳ, K., et al., 2021. The role of the vegetation structure, primary productivity and senescence derived from airborne LiDAR and hyperspectral data for birds diversity and rarity on a restored site. Landsc. Urban Plan. 210, 104064.

Olmo, V., Tordoni, E., Petruzzellis, F., Bacaro, G., Altobelli, A., 2021. Use of sentinel-2 satellite data for windthrows monitoring and delimiting: the case of "Vaia" storm in friuli venezia Giulia region (north-eastern Italy). Remote Sens. 13 (8), 1530.

Perrone, M., Conti, L., Galland, T., Komárek, J., Lagner, O., Torresani, M., Rossi, C., Carmona, C.P., de Bello, F., Rocchini, D., et al., 2024. "Flower power": How flowering affects spectral diversity metrics and their relationship with plant diversity. Ecol. Inform. 81, 102589.

Pettorelli, N., Schulte to Bühne, H., Tulloch, A., Dubois, G., Macinnis-Ng, C., Queirós, A.M., Keith, D.A., Wegmann, M., Schrodt, F., Stellmes, M., et al., 2018. Satellite remote sensing of ecosystem functions: opportunities, challenges and way forward. Remote Sens. Ecol. Conserv. 4 (2), 71–93.

Pilli, R., Vizzarri, M., Chirici, G., 2021. Combined effects of natural disturbances and management on forest carbon sequestration: the case of vaia storm in Italy. Ann. Forest Sci. 78 (2), 46.

Polychronaki, A., Spindler, N., Schmidt, A., Stoinschek, B., Zebisch, M., Renner, K., Sonnenschein, R., Notarnicola, C., 2015. Integrating RapidEye and ancillary data to map alpine habitats in south Tyrol, Italy. Int. J. Appl. Earth Obs. Geoinf. 37, 65–71.

R Core Team, 2000. R Language Definition. Vol. 3, R Foundation for Statistical Computing, Vienna, Austria, 1.

Rahman, M.F., Onoda, Y., Kitajima, K., 2022. Forest canopy height variation in relation to topography and forest types in central Japan with LiDAR. Forest Ecol. Manag. 503, 119792.

Ricotta, C., 2005. Additive partitioning of Rao's quadratic diversity: a hierarchical approach. Ecol. Model. 183 (4), 365–371.

Ricotta, C., Carranza, M.L., 2013. Measuring scale-dependent landscape structure with Rao's quadratic diversity. ISPRS Int. J. Geo-Inf. 2 (2), 405–412.

Ricotta, C., Marignani, M., 2007. Computing β-diversity with Rao's quadratic entropy: a change of perspective. Diversity and Distributions 13 (2), 237–241.

Rocchini, D., Marcantonio, M., Da Re, D., Chirici, G., Galluzzi, M., Lenoir, J., Ricotta, C., Torresani, M., Ziv, G., et al., 2019. Time-lapsing biodiversity: An open source method for measuring diversity changes by remote sensing. Remote Sens. Environ. 231, 111192–1.

Rocchini, D., Marcantonio, M., Ricotta, C., 2017. Measuring Rao's Q diversity index from remote sensing: An open source solution. Ecol. Indic. 72, 234–238.

Rocchini, D., Thouverai, E., Marcantonio, M., Iannacito, M., Da Re, D., Torresani, M., Bacaro, G., Bazzichetto, M., Bernardi, A., Foody, G.M., et al., 2021. Rasterdiv—An information theory tailored R package for measuring ecosystem heterogeneity from space: To the origin and back. Methods Ecol. Evol. 12 (6), 1093–1102.

Rocchini, D., Torresani, M., Beierkuhnlein, C., Feoli, E., Foody, G.M., Lenoir, J., Malavasi, M., Moudrỳ, V., Šímová, P., Ricotta, C., 2022. Double down on remote sensing for biodiversity estimation: a biological mindset. Commun. Ecol. 23 (3), 267–276.

Rocchini, D., Torresani, M., Ricotta, C., 2024. On the mathematical properties of spatial Rao's Q to compute ecosystem heterogeneity. Theor. Ecol. 1–8.

Seidl, R., Thom, D., Kautz, M., Martin-Benito, D., Peltoniemi, M., Vacchiano, G., Wild, J., Ascoli, D., Petr, M., Honkaniemi, J., et al., 2017. Forest disturbances under climate change. Nat. Clim. Change 7 (6), 395–402.

Senf, C., Müller, J., Seidl, R., 2019. Post-disturbance recovery of forest cover and tree height differ with management in central Europe. Landsc. Ecol. 34 (12), 2837–2850.

Tamburlin, D., Torresani, M., Tomelleri, E., Tonon, G., Rocchini, D., 2021. Testing the height variation hypothesis with the R rasterdiv package for tree species diversity estimation. Remote Sens. 13 (18), 3569.

Thouverai, E., Marcantonio, M., Lenoir, J., Galfré, M., Marchetto, E., Bacaro, G., Gatti, R.C., Da Re, D., Di Musciano, M., Furrer, R., et al., 2022. Integrals of life: Tracking ecosystem spatial heterogeneity from space through the area under the curve of the parametric Rao's Q index. Ecol. Complex. 52, 101029.

Tomppo, E., Ronoud, G., Antropov, O., Hytönen, H., Praks, J., 2021. Detection of forest windstorm damages with multitemporal sar data—A case study: Finland. Remote Sens. 13 (3), 383.

Torresan, C., Carotenuto, F., Chiavetta, U., Miglietta, F., Zaldei, A., Gioli, B., 2020. Individual tree crown segmentation in two-layered dense mixed forests from UAV LiDAR data. Drones 4 (2), 10.

Torresani, M., Kleijn, D., de Vries, J.P.R., Bartholomeus, H., Chieffallo, L., Gatti, R.C., Moudrỳ, V., Da Re, D., Tomelleri, E., Rocchini, D., 2023a. A novel approach for surveying flowers as a proxy for bee pollinators using drone images. Ecol. Indic. 149, 110123.

Torresani, M., Masiello, G., Vendrame, N., Gerosa, G., Falocchi, M., Tomelleri, E., Serio, C., Rocchini, D., Zardi, D., 2022. Correlation analysis of evapotranspiration, emissivity contrast and water deficit indices: A case study in four eddy covariance sites in Italy with different environmental habitats. Land 11 (11), 1903.

Torresani, M., Rocchini, D., Alberti, A., Moudrỳ, V., Heym, M., Thouverai, E., Kacic, P., Tomelleri, E., 2023b. LiDAR GEDI derived tree canopy height heterogeneity reveals patterns of biodiversity in forest ecosystems. Ecol. Inform. 76, 102082.

Torresani, M., Rocchini, D., Ceola, G., de Vries, J.P.R., Feilhauer, H., Moudrỳ, V., Bartholomeus, H., Perrone, M., Anderle, M., Gamper, H.A., et al., 2024a. Grassland vertical height heterogeneity predicts flower and bee diversity: an UAV photogrammetric approach. Sci. Rep. 14 (1), 809.

Torresani, M., Rocchini, D., Sonnenschein, R., Zebisch, M., Hauffe, H.C., Heym, M., Pretzsch, H., Tonon, G., 2020. Height variation hypothesis: a new approach for estimating forest species diversity with CHM LiDAR data. Ecol. Indic. 117, 106520.

Torresani, M., Rossi, C., Perrone, M., Hauser, L.T., Féret, J.-B., Moudrỳ, V., Simova, P., Ricotta, C., Foody, G.M., Kacic, P., et al., 2024b. Reviewing the spectral variation hypothesis: Twenty years in the tumultuous sea of biodiversity estimation by remote sensing. Ecol. Inform. 102702.

Udali, A., Andrighetto, N., Grigolato, S., Gatto, P., 2021. Economic impacts of forest storms—Taking stock of after-vaia situation of local roundwood markets in northeastern italy. Forests 12 (4), 414.

Ummenhofer, C.C., Meehl, G.A., 2017. Extreme weather and climate events with ecological relevance: a review. Phil. Trans. R. Soc. B 372 (1723), 20160135.

Vaglio Laurin, G., Puletti, N., Tattoni, C., Ferrara, C., Pirotti, F., 2021. Estimated biomass loss caused by the vaia windthrow in northern Italy: Evaluation of active and passive remote sensing options. Remote Sens. 13 (23), 4924.

Valinger, E., Elfving, B., Mörling, T., 2000. Twelve-year growth response of scots pine to thinning and nitrogen fertilisation. Forest Ecol. Manag. 134 (1–3), 45–53.